

# Orbital variability of the optical polarization of $\gamma$ -ray binary LS I +61 303



Vadim Kravtsov<sup>1</sup>, A. Berdyugin, V. Pirola, I. Kosenkov, S. Tsygankov, M. Chernyakova, D. Malyshev, T. Sakanoi, M. Kagitani, S. Berdyugina, J. Poutanen

<sup>1</sup> University of Turku, Finland, vakrau@utu.fi

Kravtsov et al., A&A 643, A170 (2020)

## Abstract

We present the results of BVR polarimetric and photometric observations of the  $\gamma$ -ray binary LS I +61 303, performed from November 2016 to January 2019. We detect statistically significant variability of the Stokes parameters with a period  $P = 13.25^d$ , close to half of the orbital period  $P_{\text{orb}} = 26.496^d$ . Using a model of Thomson scattering by a cloud that orbits the Be star, we obtained constraints on the orbital parameters, including a small eccentricity  $e < 0.2$  and periastron phase of  $\phi_p \approx 0.6$ , which coincides with the peaks in the radio, X-ray, and TeV emission. By folding the photometry data acquired during a three-year time span with the orbital period, we found a linear phase shift of the moments of the brightness maximum, confirming the possible existence of superorbital variability.

## Optical polarimetry

We observed LS I +61 303 with the polarimeter Dipol-2 (Pirola et al., 2014) mounted on the 2.2 m UH88 telescope at Mauna Kea Observatory and the 60 cm Tohoku telescope (T60) at Haleakala Observatory, Hawaii during 140 nights.

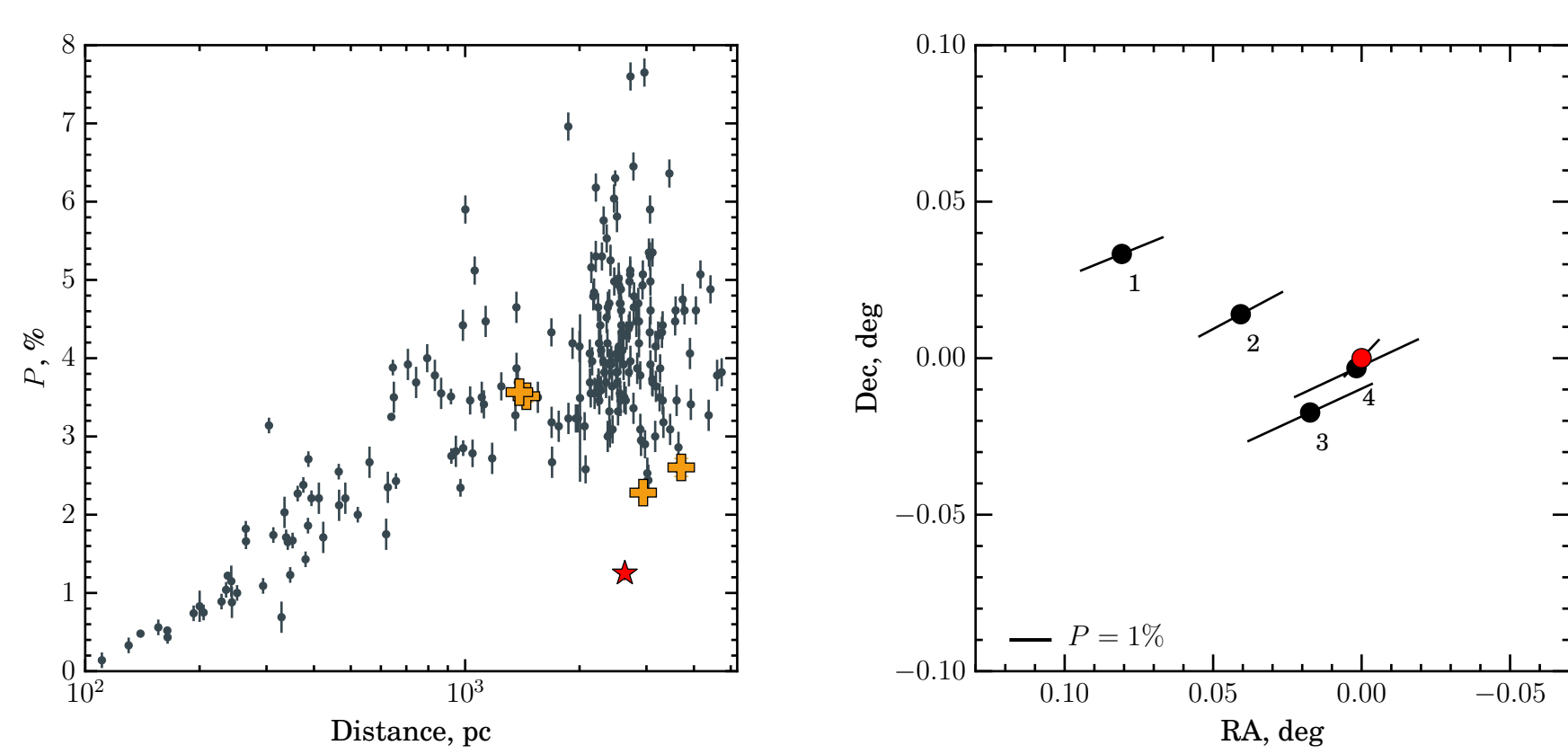


**Figure 1:** Left panel: dependence of the observed polarization  $P$  on distance for LS I +61 303 (red star), field stars (orange crosses), and for stars in the  $10^\circ \times 10^\circ$  area around LS I +61 303 (Heiles, 2000). Right panel: polarization map of LS I +61 303 (red circle at the origin) and field stars (black circles) in the  $R$  band.

Using the polarimetric measurements of the field stars (Fig. 1), we determined the interstellar polarization and hence the intrinsic polarization of LS I +61 303 (see Tab. 1).

Filter	Observed		Intrinsic	
	$P_{\text{obs}}$ (%)	$\theta_{\text{obs}}$ (deg)	$P_{\text{int}}$ (%)	$\theta_{\text{int}}$ (deg)
$B$	$1.14 \pm 0.05$	$139.5 \pm 1.5$	$1.66 \pm 0.07$	$13.5 \pm 0.9$
$V$	$1.21 \pm 0.05$	$136.4 \pm 1.2$	$1.72 \pm 0.05$	$10.8 \pm 0.7$
$R$	$1.25 \pm 0.04$	$135.4 \pm 1.0$	$1.66 \pm 0.05$	$8.4 \pm 0.7$

**Table 1:** Intrinsic polarization of the LS I +61 303.

We found periodic variability of the polarization with the period of  $P = 13.25^d$  which, taking into account measurement errors, is equal to the half of the orbital period  $P_{\text{orb}} = 26.496^d$ . Folding the data with the orbital period we got the orbital lightcurves of the polarization (Fig. 2).

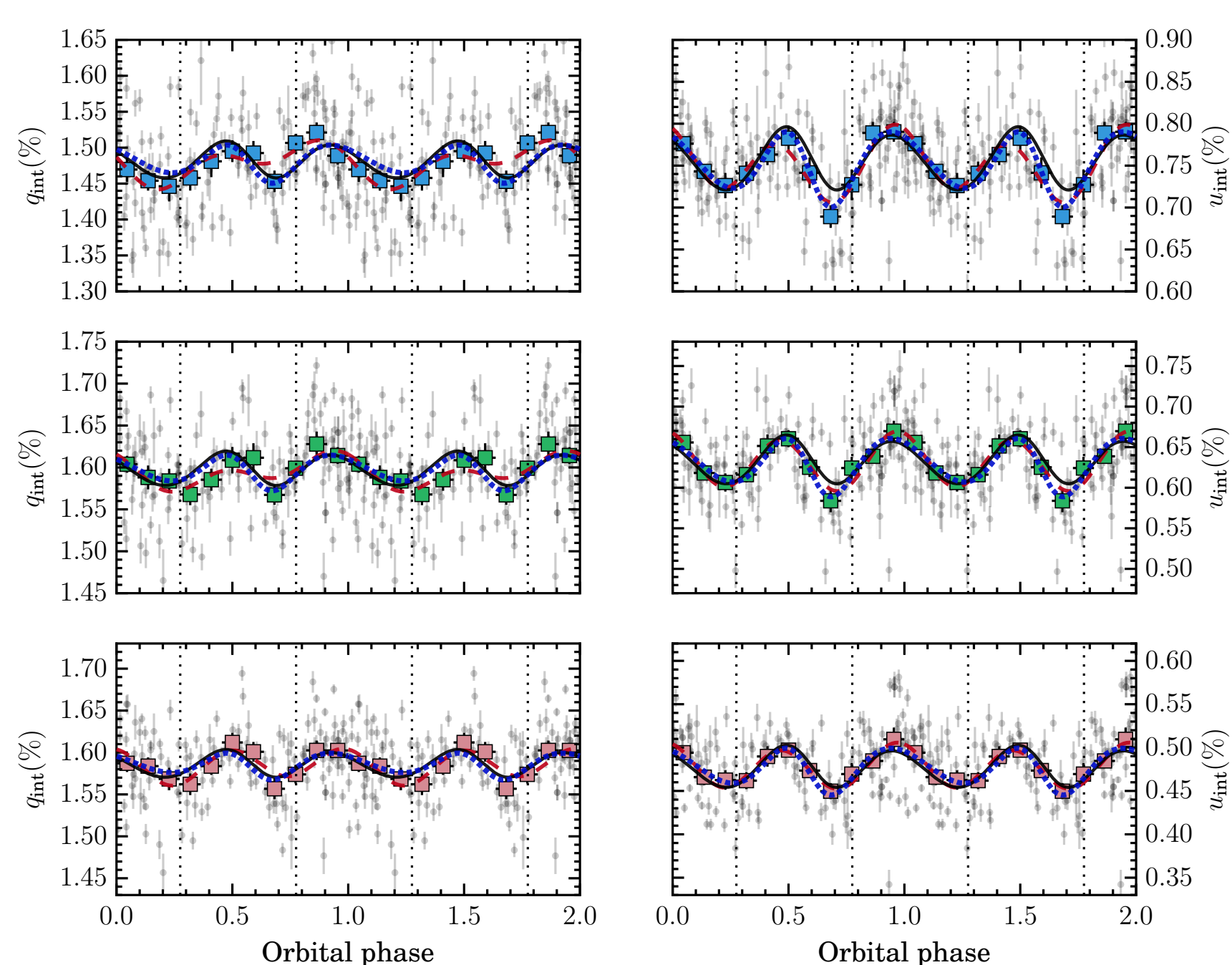


**Figure 2:** Phase curves for Stokes  $q$  (left column) and  $u$  (right column) in  $B$ ,  $V$  and  $R$  bands (top, middle and bottom panel correspondingly). Vertical dashed lines corresponds to the phases of periastron ( $\varphi = 0.275$ ) and apastron ( $\varphi = 0.775$ ).

Using a model of a scattering cloud at an elliptical orbit nearly coplanar with the disk, we modeled orbital variations of Stokes parameters and constrained the eccentricity at  $e < 0.15$  and the phase of the periastron at  $\varphi_p \approx 0.6$ . (see Tab. 2, Fig. 3, Fig. 4)

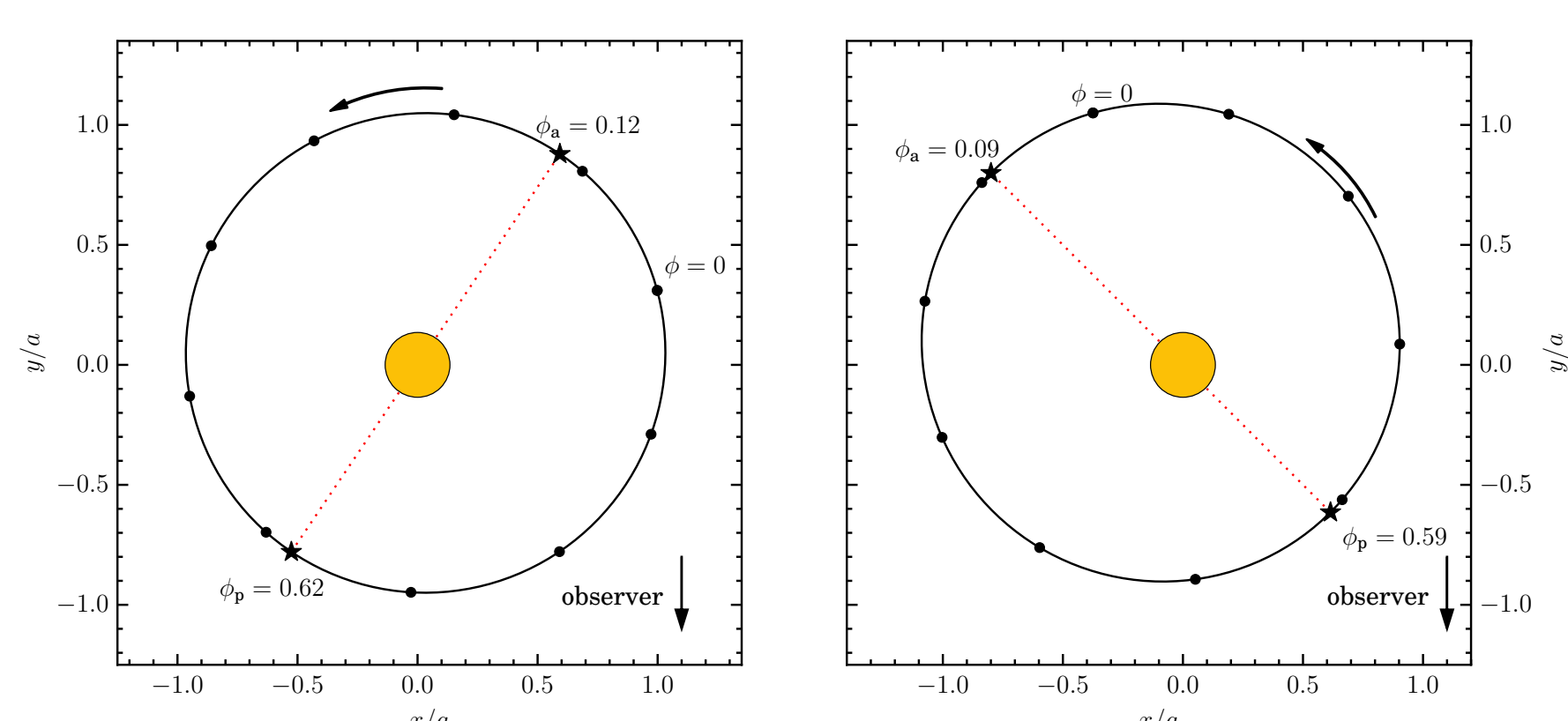


**Figure 3:** Relative orbit of a compact object in LS I +61 303 around Be star (yellow circle at the origin), which lies at the ellipse focus. The orbital parameters are taken from Tab. 2. Left panel: orbit for constrained orientation relative to the decretion disk plane with  $\Omega = \theta_{\text{int}} \pm 10^\circ$ . Right panel: orbit assuming free  $\Omega$ .

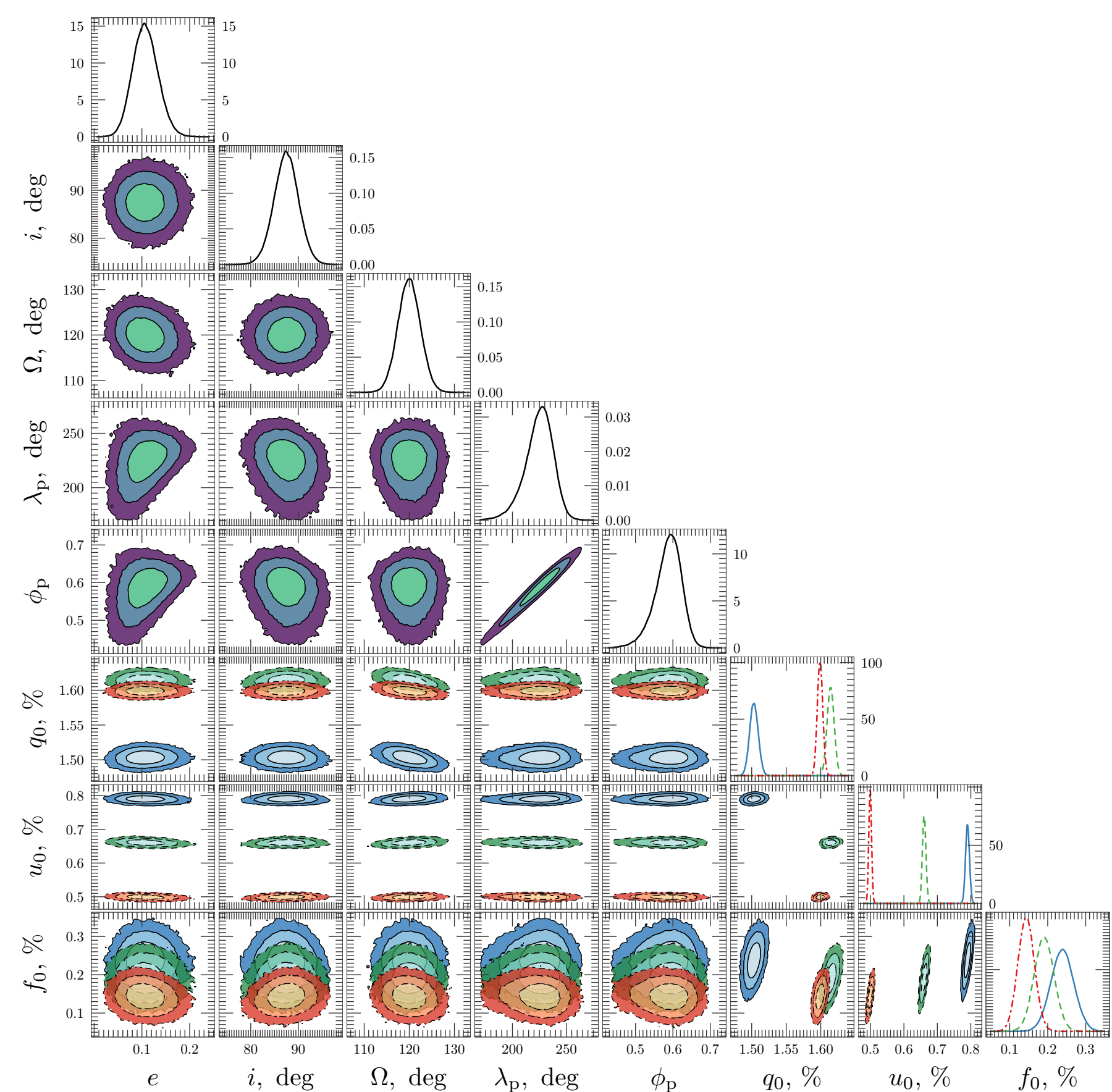


**Figure 4:** Posterior distributions for parameters of model.

We note that the inclination of the orbit, derived from the polarimetric observations modeling, is biased towards a higher value, while the obtained values of the eccentricity and the periastron phase are quite robust.

	$e$	$i$ (deg)	$\Omega$ (deg)	$\lambda_p$ (deg)	$\phi_p$
$\Omega = \theta_{\text{int}} \pm 10^\circ$	$0.06 \pm 0.02$	$86 \pm 3$	$28 \pm 3$	$146 \pm 22$	$0.62 \pm 0.07$
Free $\Omega$	$0.11 \pm 0.03$	$87 \pm 3$	$120 \pm 2$	$225 \pm 13$	$0.59 \pm 0.04$

**Table 2:** Best fit orbital parameter estimates. Errors are  $1\sigma$ .

## Optical photometry

In addition to polarimetry, we were able to do photometric studies of the  $\gamma$ -ray binary LS I +61 303.

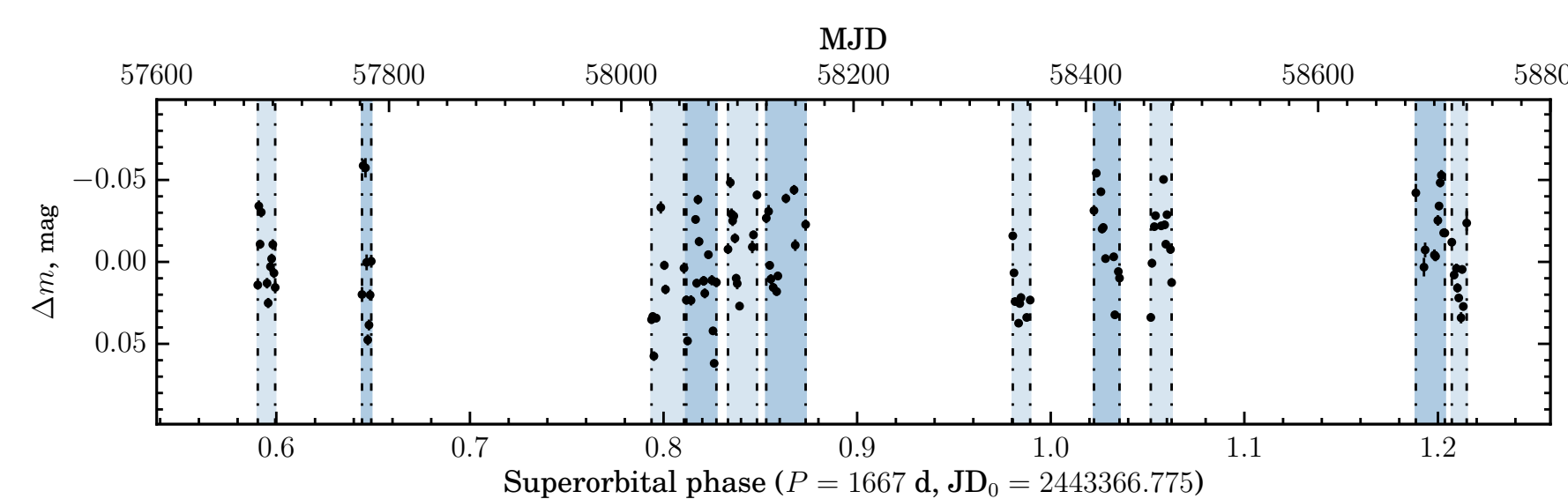


**Figure 5:** Variation of relative amplitude of LS I +61 303 around the mean in the  $V$  passband as a function of superorbital phase. The shaded blue bands correspond to the eleven observing seasons (S1–S11).

We folded our photometric data with the orbital period and plotted phase curves of brightness variability in  $BVR$  filters (Fig. 6). One might note the big amount of scatter in the data. To examine the nature of this scatter, we split the data set on 11 full orbital cycles (S1–S11) and fit them with the function  $m(\phi) = -A \cos[2\pi(\phi - \phi_0)] + m_0$ , where  $\phi_0$  (phase of the peak),  $A$  (amplitude), and  $m_0$  (vertical offset) are free parameters (see Fig. 7).

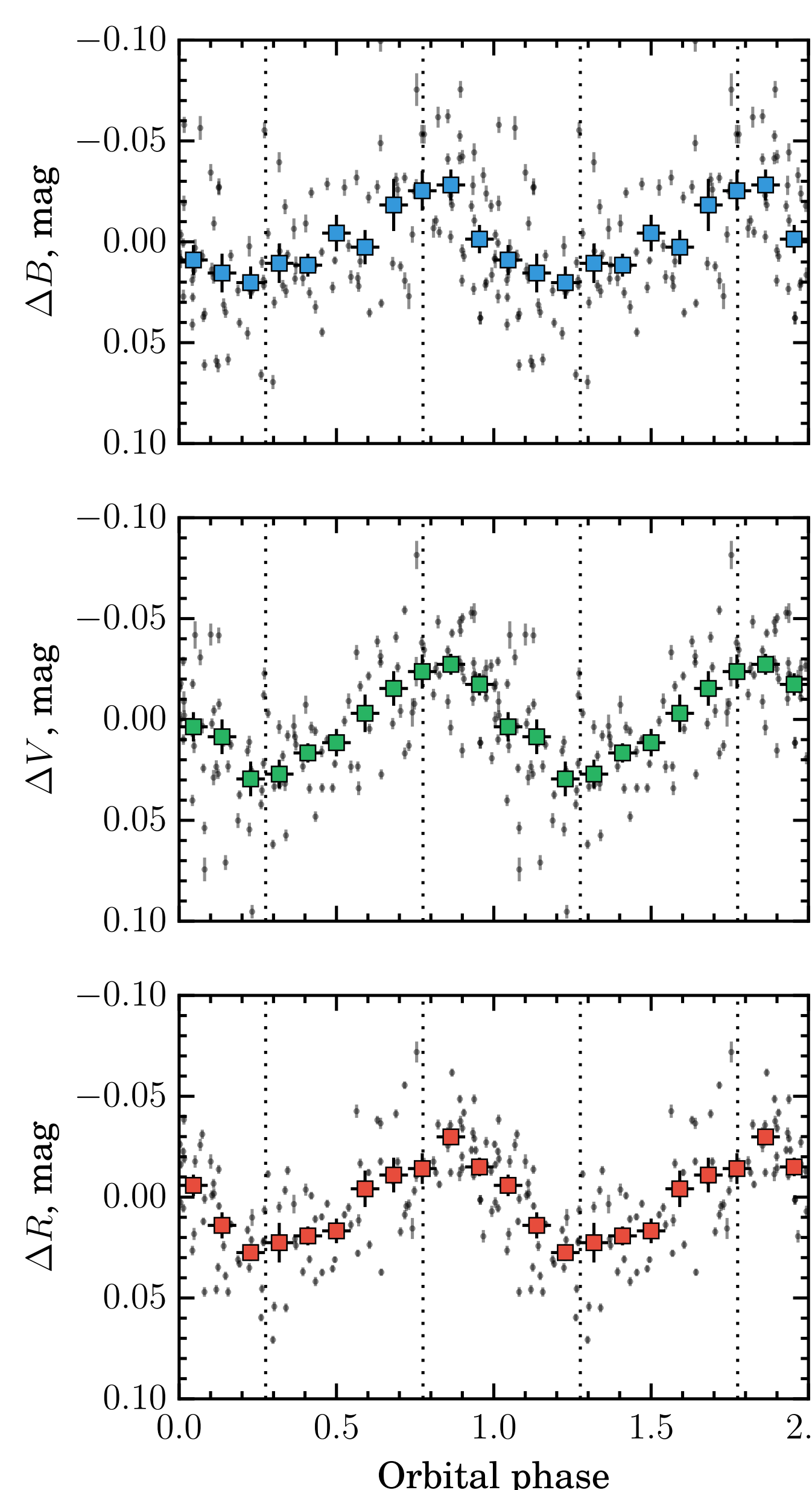


**Figure 6:** Variability of LS I +61 303 brightness in  $BVR$  bands (top, middle, and bottom panels, respectively) with the orbital period. The filled squares with  $1\sigma$  errors correspond to the average values of the individual observations (gray crosses) and the standard errors of the mean calculated within the phase bin of width  $\Delta\phi = 0.091$ .

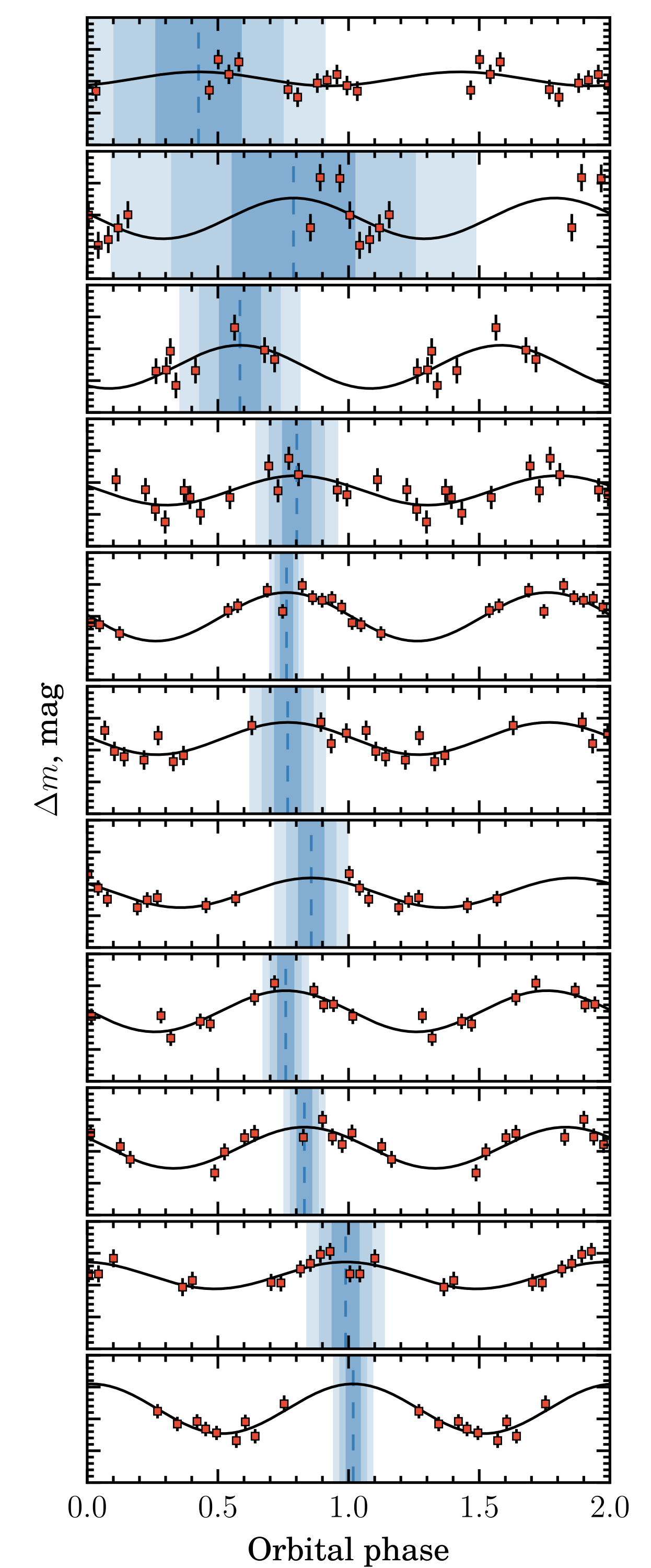


**Figure 7:** Variability of LS I +61 303 optical brightness in  $V$ -band for different orbital cycles (S1–S11, from top to bottom). The vertical dashed lines give the phases of the best fit maxima  $\phi_0$ , and the corresponding  $\pm 1\sigma$ ,  $\pm 2\sigma$ , and  $\pm 3\sigma$  confidence intervals are shown with varying shades of blue. The vertical scale  $[0.1, -0.1]$  is the same in all panels.

We found the linear shift of the phase of the maximum of brightness with superorbital phase (upper panel of Fig. 8), which causes the scatter on the orbital light curve.

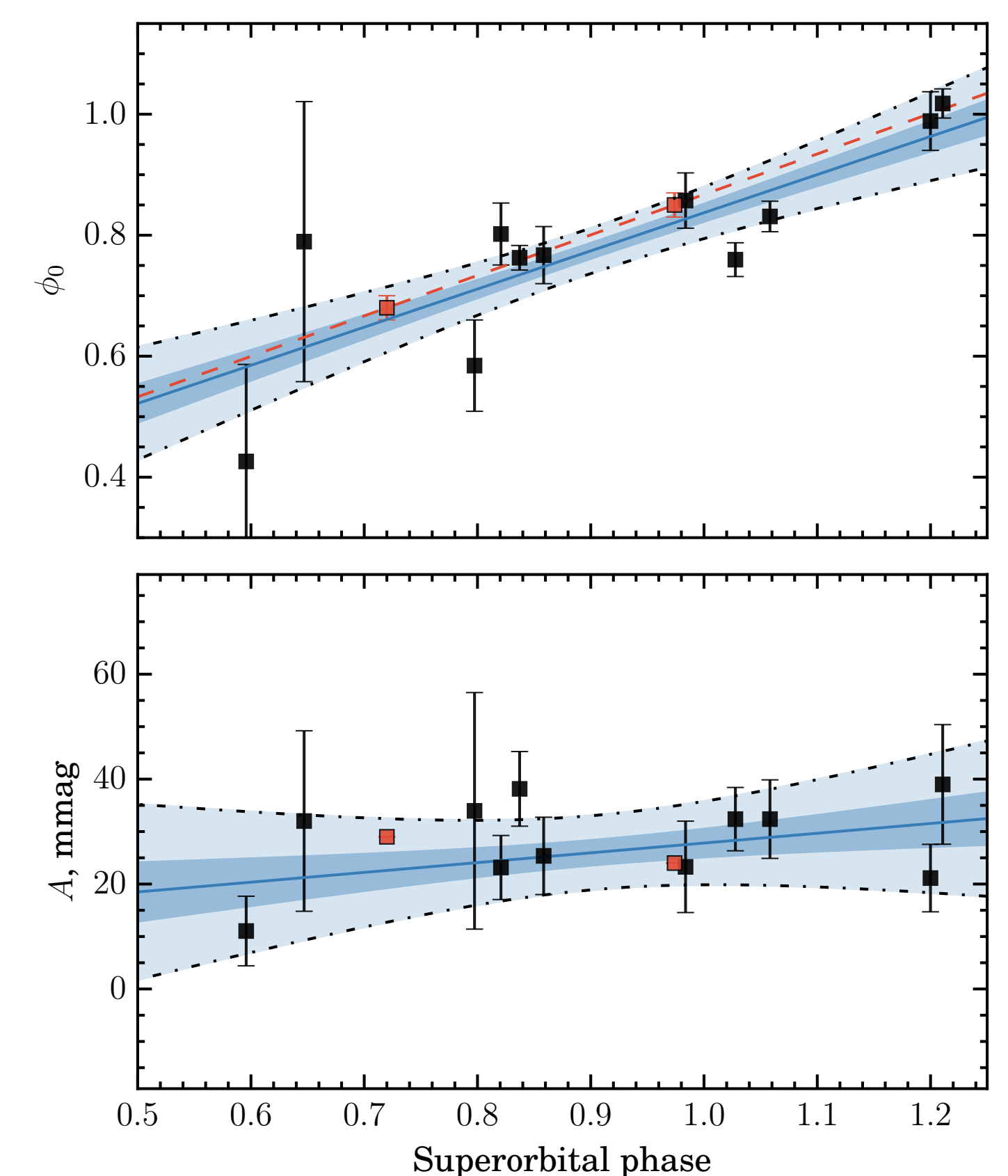


**Figure 8:** Dependence of brightness maximum orbital phase  $\phi_0$  (top panel) and the amplitude  $A$  (bottom panel) of the sinusoidal fits on the superorbital phase. The solid blue lines correspond to the linear fit of the data, while the  $\pm 1\sigma$  and  $\pm 3\sigma$  confidence intervals are shown in dark and light blue. The red squares show the parameters from Table 3 of Paredes-Fortuny et al., 2015.

## Conclusions

Our high-precision  $BVR$  measurements of the linear polarization of the  $\gamma$ -ray binary LS I +61 303 revealed periodic orbital variability in all passbands. The timing analysis of the Stokes parameters yielded the first ever detection of a polarimetric period  $P_{\text{pol}} = 13.244$  d, which is close to half of the orbital period  $P_{\text{orb}} = 26.496$  d. The mechanism producing orbital variation of the polarization is most likely Thomson scattering of the stellar light in the high-temperature region around the compact object. Using a model of Thomson scattering by a cloud that orbits the Be star at an elliptical orbit, we modeled orbital variations of Stokes parameters and constrained the eccentricity at  $e < 0.15$  and the phase of the periastron at  $\varphi_p \approx 0.6$ . The obtained value for the periastron phase differs significantly from the previously assumed phase, which is based on the RV measurements, but is very close to the peaks of the radio, X-ray, and TeV light curves. We also found photometric orbital variability of LS I +61 303 in  $B$ ,  $V$ , and  $R$  filters with amplitudes  $\Delta m \approx 0.1$  mag. The phase shift of the brightness maximum between the data sets acquired over the period of three years can be approximated with a simple linear model. Our results thus open a new avenue to model the broad-band emission from the enigmatic  $\gamma$ -ray binary LS I +61 303.